Magnetic properties of mixed ferro-ferrimagnets composed of Prussian blue analogs

Shin-ichi Ohkoshi* and Tomokazu Iyoda†
Kanagawa Academy of Science and Technology (KAST), 1583 Iiyama, Atsugi, Kanagawa 243-02, Japan

Akira Fujishima‡ and Kazuhito Hashimoto*,‡
Kanagawa Academy of Science and Technology (KAST), 1583 Iiyama, Atsugi, Kanagawa 243-02, Japan
and Department of Applied Chemistry, Faculty of Engineering, The University of Tokyo, Hongo, Bunkyo-ku, Tokyo 113, Japan
(Received 22 April 1997)

We have succeeded in controlling the saturation magnetization (I_S), the Weiss temperature (θ), and the coercive field (H_c) using compounds in the series $(Ni^{II}_xMn^{II}_{1-x})_{1.5}[Cr^{III}(CN)_6]$ as model compounds. The key to this strategy is to manipulate both ferromagnetic ($J>0$) and antiferromagnetic ($J<0$) exchange interactions by incorporating the appropriate molar ratios of the transition-metal ions. Minimum values of I_S were found for x values close to 3/7 (0.429), just at the point where parallel spins (Cr^{III} and Ni^{II}) and antiparallel spins (Mr^{II}) should completely cancel out. The θ_c values increased monotonically from negative to positive with increasing x, indicating that the predominant interaction mode was shifting from antiferromagnetic to ferromagnetic. The highest coercive field was observed for a compound with an x value close to 3/7. The magnetization vs temperature curves below T_c exhibited various types of behavior, depending on x. For example, the curves for $x=0$ and $x=1$ exhibited monotonic increases in magnetization below T_c with decreasing T, while the curve for $x=0.45$ exhibited a single maximum, and that for $x=0.38$ exhibited two maxima in a field of 1000 G. Of particular interest is the fact that the compound for which x was 0.38 exhibited negative values of magnetization in a field of 10 G below approximately 39 K and positive values above this temperature, showing that the magnetic pole can be inverted. We analyzed these temperature dependences using molecular-field theory with three types of sublattice (Ni, Mn, Cr) sites. This phenomenon is observed because the negative magnetization due to the Mn^{II} sublattice and the positive magnetizations due to the Ni^{II} and Cr^{III} sublattices have different temperature dependences. [S0163-1829(97)05042-X]

I. INTRODUCTION

In general, materials which exhibit strong bulk magnetization can be roughly divided into two categories, ferromagnets (parallel spin ordering) and ferrimagnets (antiparallel ordering of unlike spins). Our objective in the present work is to gain understanding of a new type of molecule-based magnet, the mixed ferro-ferrimagnet, which has both a ferromagnetic and ferrimagnetic character. It may be difficult to achieve such properties in metal-oxide magnets because various types of magnetic interactions involving the metal ions can operate in these systems, including superexchange interactions, direct exchange interactions, and dipole-dipole interactions. Instead, we have chosen Prussian blue analogs as target materials. These materials comprise one of the more attractive classes of molecule-based magnets,[1–3] some with high critical temperatures (T_c).[4–7] For example, Verdaguer *et al.* reported $V[Cr(CN)_6]_{0.86}\cdot 2.8\,H_2O$, which exhibits the highest critical temperature ($T_c=315$ K) among the Prussian blue analogs.[7] In addition, Prussian blue analogs are useful for the molecular design of magnetic properties because various types of metal ions can be easily incorporated as spin centers.[4–14] Their common fcc structure allows us to easily understand the superexchange interactions between the neighboring metal ions through the cyanide bridging ligands. Depending on the types of metal ions incorporated, these materials show either ferromagnetism or ferrimagnetism.

As prototypes exemplifying our concept of the mixed ferro-ferrimagnet, we recently synthesized a series of $(Ni^{II}_xMr^{II}_{1-x})_{1.5}[Cr^{III}(CN)_6]$ compounds, which can accommodate both ferromagnetic ($J>0$) and antiferromagnetic ($J<0$) exchange interactions. Their magnetic properties, such as saturation magnetization (I_S), Weiss temperature (θ), and coercive field (H_c), can be controlled by changing the compositional factor x.[15] In addition, we have also demonstrated various types of temperature dependences of the magnetization by changing x. In most cases, the spontaneous magnetization increases monotonically with decreasing temperature below T_c. However, in the classical theory of ferrimagnets, Néel envisaged the possibility that the spontaneous magnetization might change sign, i.e., magnetic pole inversion, at a particular temperature (compensation temperature, T_{comp}).[16] In fact, several magnetic materials, such as $NiFe_{2-x}V_xO_4$ and $Li_{0.5}Fe_{2.5-x}Al_xO_4$, exhibiting negative magnetization have been found.[17–20] Recently, in the field of molecular-based magnets, Mathoniére *et al.* and Re *et al.* have reported that $NBu_4[Fe^{II}Fe^{III}(C_2O_4)_3]$ and $[K\{Mn(3\text{-MeO-salen})\}_2\{Mn(CN)_6\}]$ [3-MeC-salen =N,N′-ethylenebis(3-methoxy salicylideneaminato)] show negative magnetization, although the mechanisms have not yet been elucidated.[21–23] In the present work, we have been able to design magnets exhibiting negative magnetization by fine tuning the composition. The temperature dependence of the magnetization can be explained using molecular-field theory. Moreover, in a mixed ferro-ferrimagnet $(Fe_{0.40}Mn_{0.60})_{1.5}[Cr^{II}(CN)_6]$ exhibiting negative magnetization, we have recently succeeded in demonstrating a photo-

induced magnetic pole inversion.[24] This phenomenon draws attention to the possibility of novel types of functionality for magnets.

In this paper, we report the details of the magnetic properties and theoretical treatment of this novel mixed ferro-ferrimagnetic phenomenon, attempting to answer the following questions: (1) How are the I_S values controlled in ternary metal Prussian blue analogs? (2) Why is the H_c value largest for the composition of vanishing I_S? (3) How do the θ values depend on the mixing ratio between ferromagnetic and ferrimagnetic character? (4) Why does negative magnetization appear?

II. THEORY

A. Superexchange interactions of Prussian blue analogs

Let us first consider the magnetic coupling of metals in Prussian blue analogs. The coupling is explainable neither by weak dipole-dipole interactions nor by direct exchange interactions via overlapping metal orbitals. The coupling may be described in terms of a superexchange mechanism through the cyanide ligands. The superexchange mechanism is summarized on the basis of the Goodenough-Kanamori rule,[25–27] which includes consideration of the symmetry of the metal and ligand orbitals concerned and the bond angle. There are two mechanisms for superexchange interactions: the kinetic exchange mechanism (J_{KE}) and the potential exchange mechanism (J_{PE}) [Fig. 1(a)].[10,28] On one hand, kinetic exchange is mediated by a direct pathway of the overlapping orbitals, which connect the two interacting magnetic orbitals. It is antiferromagnetic in nature as a consequence of the Pauli principle, leading to an antiparallel spin ordering via a common covalent bond. On the other hand, potential exchange is effective between orthogonal magnetic orbitals with comparable orbital energy. In this case Hund's rule leads to a parallel spin alignment, i.e., a ferromagnetic interaction. In the case of Prussian blue analogs, the metal d orbitals are split into t_{2g} and e_g sets by the CN ligands. Therefore, based on magnetic orbital symmetry, we can understand whether the superexchange interaction among metals ions is J_{KE} or J_{PE}. When the magnetic orbital symmetries of the metals are the same, the superexchange interaction is J_{KE}. Conversely, when the magnetic orbital symmetries of the metals are different, the superexchange interaction is J_{PE}.

As an example, we will consider the case of the hexacyanochromate cyanide $A^{II}_y[Cr^{III}(CN)_6]$, with Cr^{III} being $(t_{2g})^3$ and $S_{\mathrm{Cr}}=3/2$. The magnetic orbitals of Cr^{III} have t_{2g} symmetry. Therefore, there is no overlap between Cr^{III} and A^{II} magnetic orbitals, if all of the magnetic orbitals of A^{II} have e_g symmetry. In this situation, the potential exchange mechanism becomes dominant, leading to a ferromagnetic interaction between Cr^{III} and A^{II}. In fact, in $Cs^{I}Ni^{II}[Cr^{III}(CN)_6]$, with a high-spin state for Ni^{II} $[(t_{2g})^6(e_g)^2$, $S_{\mathrm{Ni}}=1]$, a ferromagnetic interaction operates between Cr^{III} and Ni^{II}.[8] However, when all of the A^{II} magnetic orbitals have t_{2g} symmetry, the overlap between the t_{2g}(A) and t_{2g}(Cr) orbitals gives rise to kinetic exchange, leading to an antiferromagnetic interaction. If both t_{2g} and e_g electrons are present on A^{II}, the superexchange coupling constant (J_{AB}) is described as the sum of the ferromagnetic ($J_{\mathrm{PE}}>0$) and antiferronagnetic ($J_{\mathrm{KE}}<0$) orbital contributions. Kinetic exchange usually operates in preference to potential exchange, i.e., $|J_{\mathrm{KE}}|>|J_{\mathrm{PE}}|$. For example, in $Cs^{I}Mn^{II}[Cr^{III}(CN)_6]$, with a high-spin state for Mn^{II} $[(t_{2g})^3(e_g)^2$, $S_{\mathrm{Mr}}=5/2]$, the interaction between Cr^{III} and Mn^{II} is antiferromagnetic, and the compound is a ferrimagnet.[9]

B. Magnetization of mixed ferro-ferrimagnets

In the Prussian blue analog $A^{II}_y[B^{III}(CN)_6]$, the carbon ends of the cyano groups are always bonded to B^{III} and the nitrogen ends are always bonded to A^{II}, and hence the A^{II} and B^{III} ions are linked in an alternating fashion. Moreover, the superexchange interaction between the second-nearest-neighbor sites, A^{II}-A^{II} and B^{III}-B^{III} [Fig. 1(b)], can be neglected because of their long distances (ca. 10 Å). Therefore, we only need to take into account a superexchange coupling between nearest-neighbor sites. Under these conditions, even if several different transition metals (A^{II}_i) are involved, the individual signs for each A^{II}_i are aligned either ferromagnetically or antiferromagnetically with respect to the B^{III} spins, depending on their exchange character [Fig. 1(c)]. Note that spin frustration does not need to be considered. Consequently, the saturation magnetization (I_S) of $A^{II}[B^{III}(CN)_6]$ at 0 K is expressed by

$$I_S=\mu_B\left|g_B S_{(B)}+y\sum_i q_i x_i S_{(\mathrm{A}_i)}\right|, \tag{1}$$

where y denotes the molar ratio of A^{II} $(=A^{II}_1+A^{II}_2+\cdots)$ to B^{III}, x_i is the mole fraction of A^{II}_i in A^{II}, q_i is the sign of the superexchange interaction ($J_{\mathrm{A}_i\mathrm{B}}$) between A^{II}_i and B^{III}, i.e., $+1$ for ferrimagnetic interactions and -1 for antiferromagnetic interactions. The g_B and g_i terms are the g factors for B^{III} and A^{II}_i, respectively. $S_{(Ai)}$ is the spin quantum number for metal A_i, and μ_B is the Bohr magneton.

In the present study, we consider the ternary metal Prussian blue analogs that are comprised of A_1, A_2, and B and which include both ferromagnetic interactions ($J_{A_1B}>0$) and ferrimagnetic interactions ($J_{A_2B}<0$). We first consider the model compounds, $N^{II}_{1.5}[Cr^{III}(CN)_6]\cdot 8\ H_2O$,[29] a ferromagnet, and $Mn^{II}_{1.5}[Cr^{III}(CN)_6]\cdot 7.5\ H_2O$,[29] a ferrimagnet. Assuming $g=2$ for Cr^{III}, Ni^{II}, and Mn^{II}, the saturation magnetization values for the two compounds for these compositions are expected to be 6 μ_B (due to parallel alignment of the spins, with $S_{\mathrm{Ni}}=1$ and $S_{\mathrm{Cr}}=3/2$) and 4.5 μ_B (due to antiparallel alignment of the spins, with $S_{\mathrm{Mn}}=5/2$ and $S_{\mathrm{Cr}}=3/2$), respectively. If powders of the two compounds are physically mixed, the total I_s will vary between 4.5 and 6 μ_B, depending on the mixing ratio. However, when the two compounds are mixed at an atomic level, i.e., $(Ni^{II}_x Mn^{II}_{1-x})_{1.5}[Cr^{III}(CN)_6]$, parallel spins ($Cr^{III}$ and Ni^{II}) and antiparallel spins (Mn^{II}) can partially or even completely cancel, depending on the mixing ratio [Fig. 1(c)]. In this manner, materials with I_s values anywhere in the range 0 to 6 μ_B may be prepared. The dependence of I_s on x can be calculated using Eq. (1). I_s is predicted to vanish for $x=3/7$,[15] and such a material should exhibit antiferromagnetic properties.

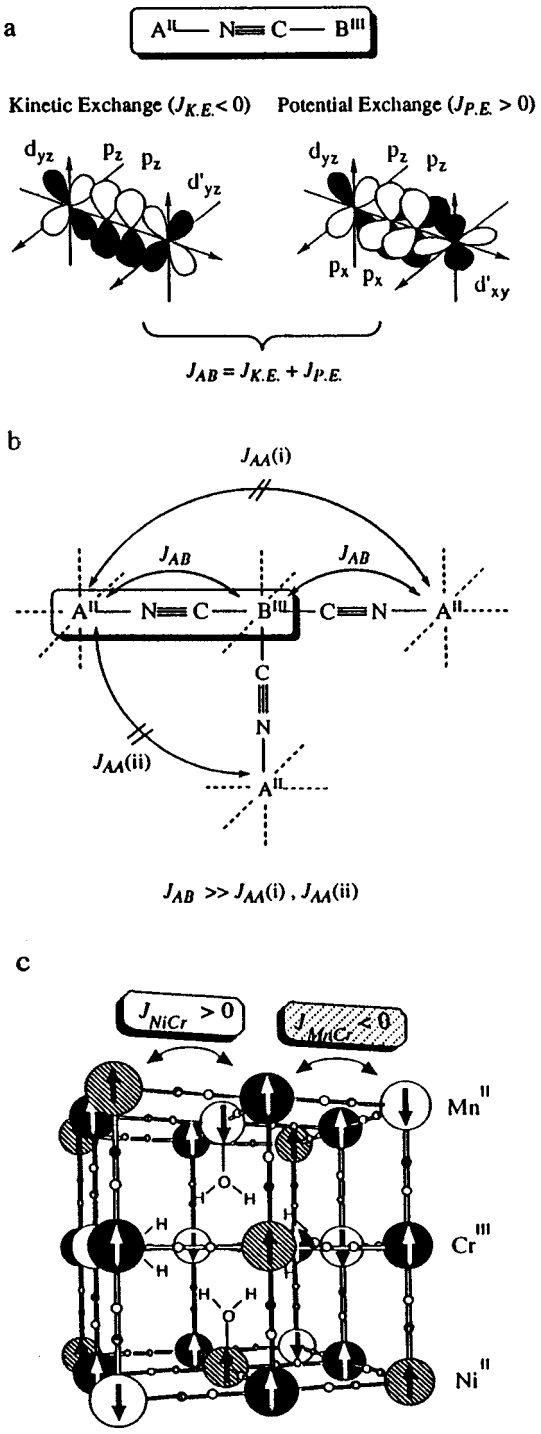

FIG. 1. (a) The two basic mechanisms for the isotropic exchange in the magnetic coupling between the A^{II} and B^{II} ions in the CN-bridged complex. On the left is one of the significant kinetic exchange (J_{KE}) pathways ($d_{yz}\|\pi_z\|d_{yz'}$) and on the right is one of significant potential exchange (J_{PE}) pathways ($d_{yz}\|\pi_z\perp\pi_x\|d_{xy'}$). The superexchange coupling between A^{II} and B^{III} (J_{AB}) involes a superposition of J_{PE} and J_{KE}. (b) In the Prussian blue structure, superexchange interactions at a 180° angle between A^{II} and B^{III} are dominant over superexchange interactions of second-nearest-neighbor metals [$J_{AA}(i)$] and direct exchange interactions [$J_{AA}(ii)$]. (c) Schematic diagram illustrating mixed ferro-ferrimagnetism with both ferromagnetic ($J_{AB}>0$) and antiferromagnetic ($J_{AB}<0$) interactions. Cr^{III} and either Ni^{II} or Mn^{II}, which are randomly incorporated in the lattice, are linked in an alternating fashion.

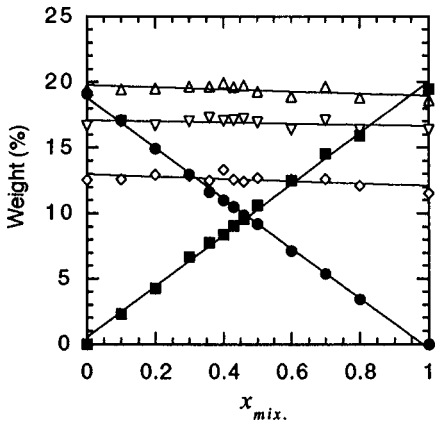

FIG. 2. Experimentally obtained weight percentages of elements vs x_{mix} for $(Ni^{II}_xMn^{II}_{1-x})_{1.5}[Cr^{III}(CN)_6]\cdot zH_2O$: (■) Ni; (●) Mn; (◇) Cr; (▽) C; (△) N.

III. EXPERIMENTAL DETAILS

A. Materials

For the preparation of the Prussian blue analogs incorporating three different metal ions, $(Ni^{II}_xMn^{II}_{1-x})_{1.5}[Cr^{III}(CN)_6]\cdot zH_2O$, a 50 cm^3 aqueous solution (0.02 mol dm^{-3}) of $NiCl_2$ and $MnCl_2$ was added to a concentrated aqueous solution (7 cm^3) of $K_3[Cr(CN)_6]$ (0.1 mol dm^{-3}), yielding a light blue colored microcrystalline powder. The precipitate was dialyzed for 48 h and then filtered. The fraction (x_{mix}) of Ni^{II} vs ($Ni^{II}+Mn^{II}$) in the above diluted aqueous solution was varied from 0 to 1, keeping the total metal ion concentration at 0.02 mol dm^{-3}. Elemental analyses for C, H, and N were carried out by standard microanalytical methods. Those for Mn, Ni, and Cr were analyzed by atomic absorption spectrometry.

B. Spectral and magnetic measurements

Infrated (IR) spectra were recorded on a Biorad Model FTS 40A spectrometer, using KBr pellets or by spreading thin layers on polyethylene sheets. UV powder reflection spectra were recorded on a Shimadzu MPC-3100 spectrometer. X-ray powder diffraction was measured on a Rigaku PW 1370 powder diffractometer. Electron paramagnetic resonance (EPR) spectra of powder samples were recorded at room temperature with a JEOL RE2X X-band EPR spectrometer. Magnetic susceptibility and magnetization measurements were carried out using a Quantum Design MPMS 7 superconducting quantum interference device magnetometer. Polycrystalline samples were loaded into gelatin capsules. To estimate the Weiss temperatures, magnetization data were collected from 150 to 300 K.

IV. RESULTS

A. Structures of $(Ni^{II}_xMn^{II}_{1-x})_{1.5}[Cr^{III}(CN)_6]\cdot zH_2O$

The elemental analyses for the synthesized complexes showed that the experimentally obtained x values were in good agreement with the x_{mix} values used in the syntheses and that the amounts of the other elements (Cr, C, N, and H) were essentially constant (Fig. 2).[30] The water content (z) depended on the humidity and temperature. Under our typi-

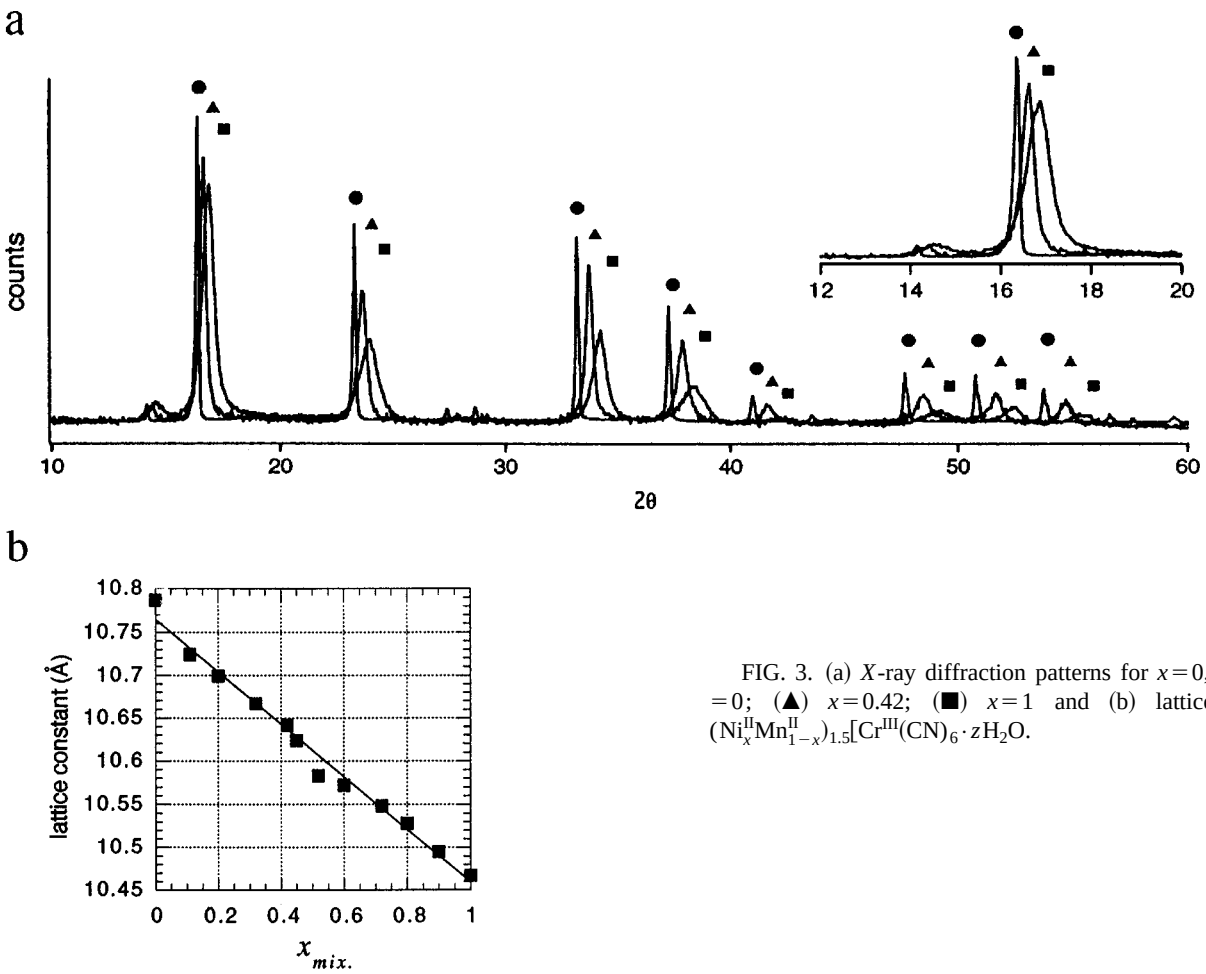

FIG. 3. (a) *X*-ray diffraction patterns for $x=0$, 0.42, 1: (●) $x=0$; (▲) $x=0.42$; (■) $x=1$ and (b) lattice constants of $(Ni_x^{II}Mn_{1-x}^{II})_{1.5}[Cr^{III}(CN)_6\cdot zH_2O$.

cal experimental conditions (humidity 70%, temperature 25 °C), z was between 7.5 and 8.

The Cr-C stretching frequencies in the IR spectra for the resulting ternary metal complexes increased continuously from 366.52 to 384.85 cm^{-1} with increasing x. Moreover, the CN stretching frequencies also increased continuously from 2160.8 to 2165.0 cm^{-1}. These observed signals can be assigned neither to manganese cyanides (Mn-CN) nor to nickel cyanides (Ni-CN) but rather to chromium cyanides (Cr-CN), and the character of the bond between the metal (Cr) and CN were successively changed depending on x.

The x-ray powder-diffraction patterns for all of the ternary complexes were consistent with the fcc structure. The x-ray powder-diffraction spectra for $x=0$, 0.42, and 1 are shown in Fig. 3(a). The lattice constant decreased successively from 10.787 to 10.467 Å with increasing x [Fig. 3(b)]. The linewidth also increased with increasing x. Conversely, when $Mn_{1.5}^{II}[Cr^{III}(CN)_6]$ $(x=0)$ and $Ni_{1.5}^{II}[Cr^{III}(CN)_6]$ $(x=1)$ powders were mixed, the peaks for both components were observed. Therefore, these materials were not physical mixtures of $Ni_{1.5}^{II}[Cr^{III}(CN)_6]$ and $Mn_{1.5}^{II}[Cr^{III}(CN)_6]$ powders but were actual ternary metal complexes, $(Ni_x^{II}Mn_{1-x}^{II})_{1.5}[Cr^{III}(CN)_6]\cdot zH_3O$, in which Mn^{II} and Ni^{II} were randomly incorporated in the lattice, corresponding to the mixing ratio of $NiCl_2$ and $MnCl_2$.

B. Magnetic properties

The EPR spectra for $Ni_{1.5}^{II}[Cr^{III}(CN)_6]\cdot 8\ H_2O$ and $Mn_{1.5}^{II}[Cr^{III}(CN)_6]\cdot 7.5\ H_2O$ were measured at room temperature in order to determine the g factors for the metal ions. The EPR spectra for each complex showed one peak, yielding either an averaged g factor for the nickel and chromium atoms ($g=2.03$) or an averaged g factor for the manganese and chromium atoms ($g=2.00$), respectively. The g values for the $(Ni_x^{II}Mn_{1-x}^{II})_{1.5}[Cr^{III}(CN)_6]\cdot zH_2O$ series increased monotonically from 2.00 to 2.03 with increasing x.

In the magnetization vs field measurements at fields up to 5 T, the saturation magnetizations, considering the g values

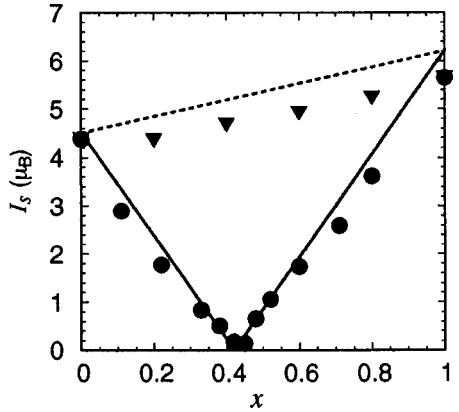

FIG. 4. Calculated and experimentally observed saturation magnetizations as a function of x. Atomic-level mixture ($(Ni_x^{II}Mn_{1-x}^{II})_{1.5}[Cr^{III}(CN)_6]\cdot zH_2O$): theory (——), observed (●). Macroscopic physical mixture ($xNi_{1.5}^{II}[Cr^{II}(CN)_6]+(1-x)Mn_{1.5}^{II}[Cr^{III}(CN)_6]$): calculated (----); observed (▼).

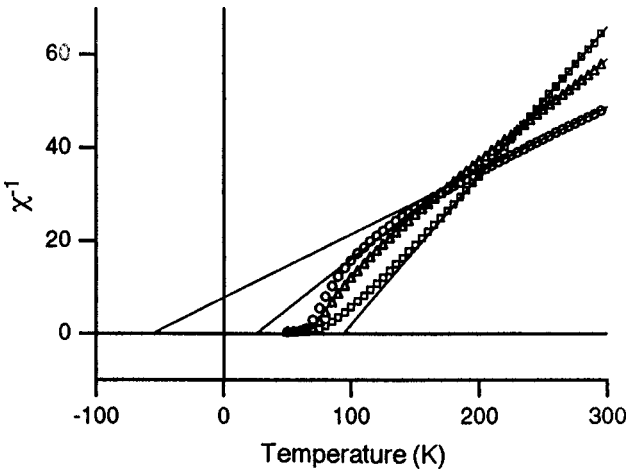

FIG. 5. Temperature dependence of the inverse magnetic susceptibility: (○) $x=0$; (△) $x=0.42$; (□) $x=1$. The magnetization data between 150 and 300 K were fitted to linear Curie-Weiss plots (——).

for $Ni^{II}_{1.5}[Cr^{III}(CN)_6]$ and $Mn^{II}_{1.5}[Cr^{III}(CN)_6]$, were determined to be 5.65 μ_B and 4.38 μ_B, respectively. When powders of the two compounds were physically mixed, I_s varied linearly between 4.38 and 5.65 μ_B, depending on the mixing ratio. In contrast, the I_s values for the $(Ni^{II}_x Mn^{II}_{1-x})_{1.5}[Cr^{III}(CN)_6 \cdot zH_3O$ series showed a systematic change as a function of x. For $0<x<3/7$, I_s decreased linearly with increasing x. In contrast, above $x=3/7$, it increased linearly with increasing x. The minimum I_s value, at x close to 3/7, was nearly zero, as seen in Fig. 4.

The magnetic susceptibilities for all of the compounds, measured in a field of 5000 G, closely obeyed the Curie-Weiss law between room temperature and 150 K (Fig. 5). The values of the Weiss temperatures (θ_c), extracted by least-squares fitting of the data, are listed in Table I. These values increased monotonically from negative values to positive values with increasing x.

The widths of the magnetic hysteresis loops for compositions in which x was close to 3/7, e.g., 0.42, were wider than those at other x values [Fig. 6(a)]. The coercive field H_c for $x\sim3/7$ was much larger than those at other x values, e.g., 6 G ($x=0$), 680 G ($x=0.42$), and 120 G ($x=1$).

TABLE I. Magnetic properties of $(Ni^{II}_x Mn^{II}_{1-x})_{1.5}[Cr^{II}(CN)_6]$.

x_{mix}	x	I_s (μ_B)	T_c (K)	θ_c (K)	H_c (G)
0	0.00	4.38 (4.42)[a]	67	−54 (−51)[a]	6 (15)[a]
0.1	0.11	2.90	67	−45	50
0.2	0.21	1.77	66	−44	120
0.3	0.33	0.84	63	−34	340
0.36	0.38	0.51	66	−28	650
0.4	0.42	0.18	68	−15	680
0.43	0.45	0.15	68	−4	540
0.5	0.52	1.06	68	1	370
0.6	0.62	1.74	69	31	160
0.7	0.71	2.59	69	42	140
0.8	0.81	3.62	70	68	120
1	1.00	5.65 (5.44)[a]	72	88 (75)[a]	120 (220)[a]

[a]Reference 29.

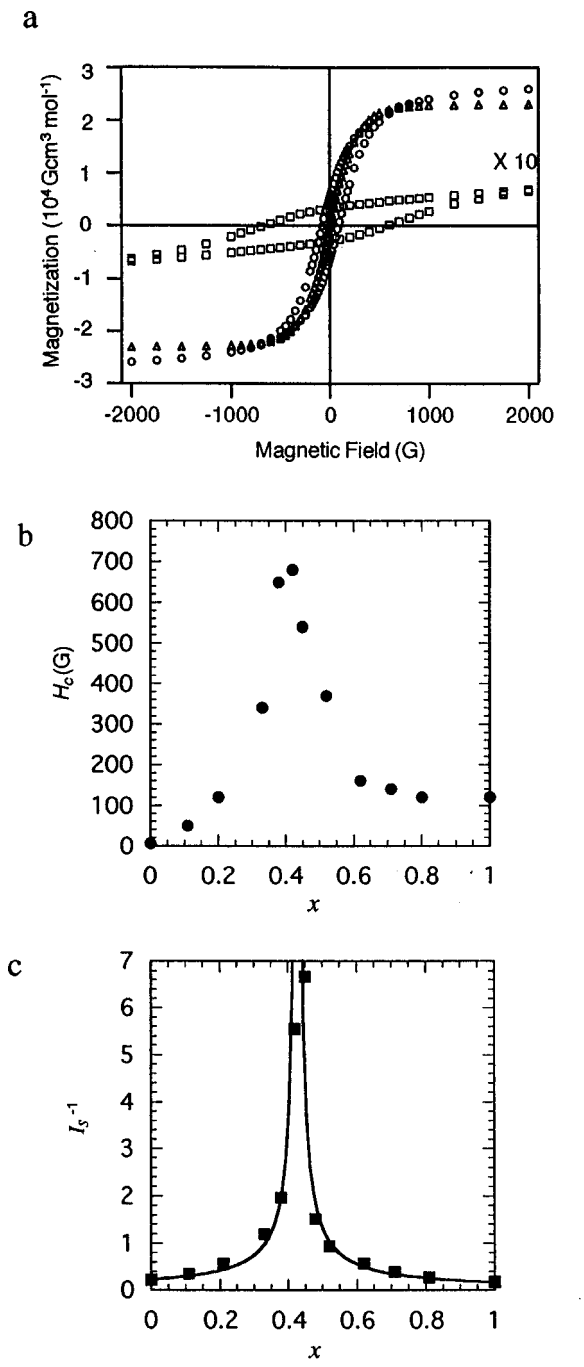

FIG. 6. (a) Hysteresis loops at 5 K for $(Ni^{II}_x Mn^{II}_{1-x})_{1.5}[Cr^{III}(Cn)_6] \cdot zH_2O$: (△) $x=0$; (□) $x=0.42$; (○) $x=1$. (b) Plots of H_c values vs x. (c) Plots of $(I_s)^{-1}$ vs x: calculated curve (——) based on Eq. (2) with $\pi\lambda\sigma=1$; observed (■)

The magnetization vs temperature curves exhibited quite interesting behavior below T_c, depending on x. For example, the curves for $x=0$ and 1 exhibited monotonic increases in magnetization with decreasing T, while the curve for $x=0.45$ exhibited a single maximum and that for $x=0.38$ exhibited two maxima (field=1000 G) [Fig. 7(a)]. In a field of 10 G, however, those compounds in which x was $0.38\sim0.42$ exhibited negative values of magnetization below particular temperatures and positive values above these values, showing that the magnetic pole can be inverted at those temperatures [Fig. 8(a)].

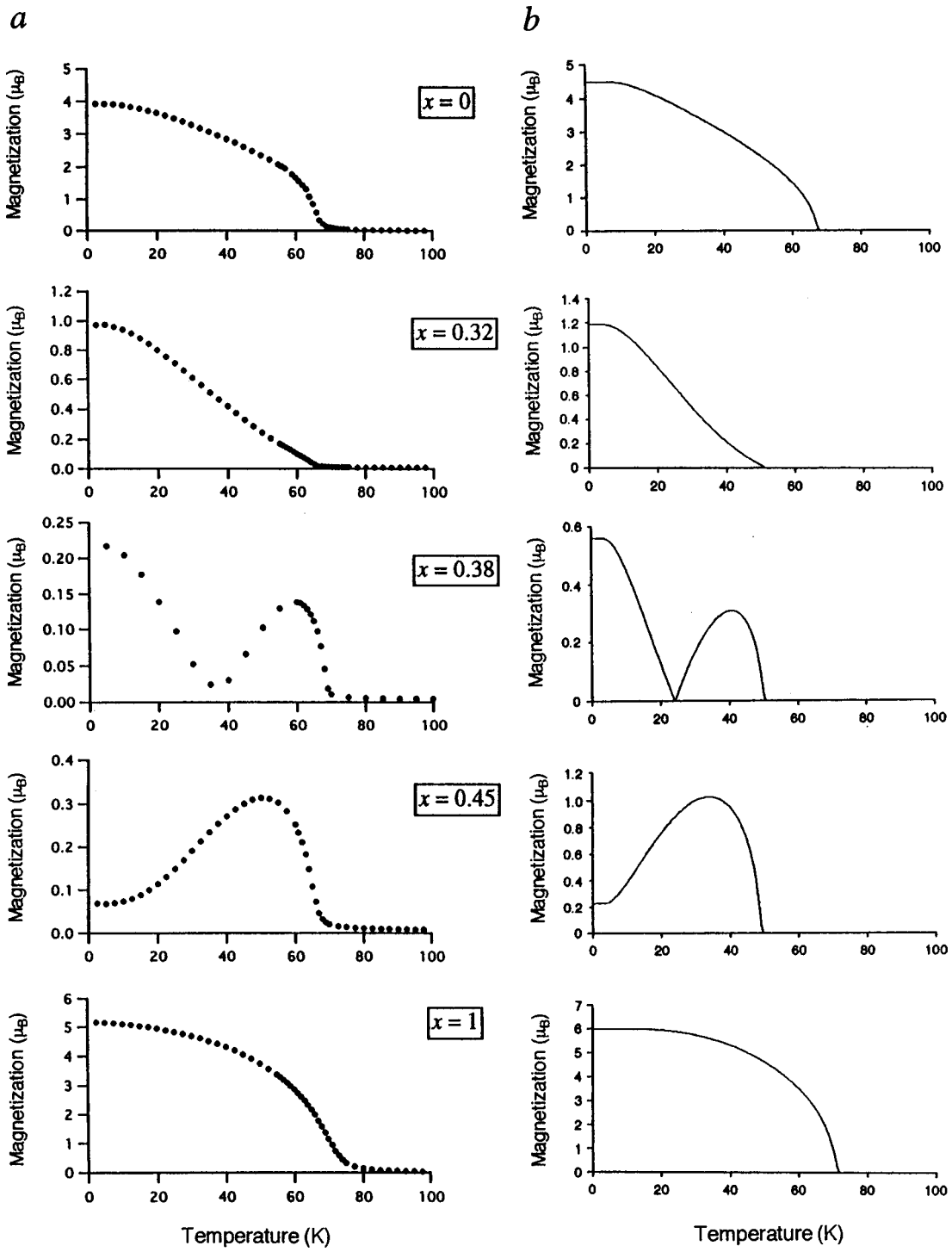

FIG. 7. Magnetization temperature curves for $(Ni_x^{II}Mn_{1-x}^{II})_{1.5}[Cr^{III}(CN)_6]\cdot zH_2O$: (a) experimental points obtained at 1000 G and (b) calculated dependence of $|M_{total}|$ based on molecular field theory, assuming three sublattices, the two J coefficients ($J_{NiCr}=5.6\ cm^{-1}$ and $J_{MnCr}=-2.5\ cm^{-1}$), and the compositional parameter x.

V. DISCUSSION

A. Saturation magnetization

The g_{Ni} and g_{Cr} values for chromium cyanides have been reported to be 2.15 and 1.99, respectively.[31] From this g_{Cr} value and the EPR data for $Cs^{I}Mn^{II}[Cr^{III}(CN)_6]$, we obtained $g_{Mn}=2.00$.[32,33] Using these g values, the spin quantum numbers for the metals ($S_{Ni}=1$, $S_{Mn}=5/2$, $S_{Cr}=3/2$), together with x, the I_s values for the members of the series $(Ni_x^{II}Mn_{1-x}^{II})_{1.5}[Cr^{III}(CN)_6]$ can be obtained using Eq. (1). The experimental I_s values were in good agreement with the calculated values (Fig. 4). In contrast, the experimental I_s values for the physically mixed powders indicate that there is negligible magnetic interaction between $Ni_{1.5}^{II}[Cr^{III}(CN)_6]$ particles and $Mn_{1.5}^{II}[Cr^{III}(CN)_6]$ particles (Fig. 4). These results suggest that our assumption is correct. That is, if the ferromagnetic and ferrimagnetic powders are physically

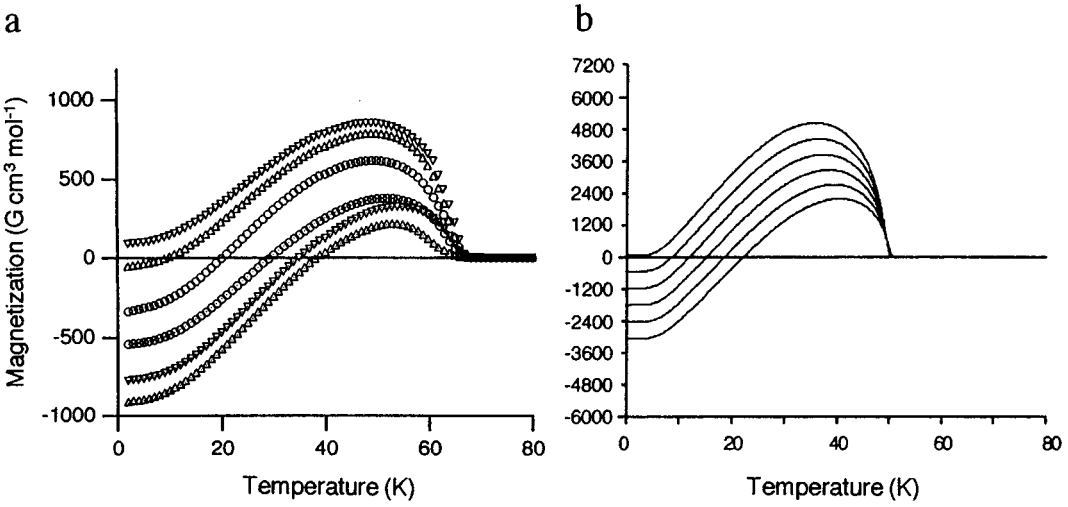

FIG. 8. Magnetization temperature curves for $(Ni_x^{II}Mn_{1-x}^{II})_{1.5}[Cr^{III}(CN)_6]\cdot zH_2O$ ($x=0.38$, 0.39, 0.40, 0.41, 0.42, and 0.43, going from lowest curve to highest curve). (a) Experimental data obtained at 10 G and (b) calculated temperature dependences of magnetization M_{total} (——) based on molecular field theory, with three sublattice sites (Ni, Mn, Cr), with J coefficients $J_{NiCr}=5.6\ cm^{-1}$ and $J_{MnCr}=-2.5\ cm^{-1}$.

mixed, the total I_s varies linearly between the respective saturation magnetization, depending on the mixing ratio. However, if the ferromagnet and ferrimagnet are mixed at an atomic level, parallel spins and antiparallel spins can partially or even completely cancel, depending on the mixing ratio.

In general, when different metal ions are substituted for one another in metal oxides such as yttrium-iron-garnet and gadolinium-iron-garnet, the estimation of the saturation magnetization is not straightforward because such substitution often induces structural changes. In our system, however, the saturation magnetization is controlled at will, according to theory, simply by varying x from 0 to 1. One of the reasons for this is that, with Prussian blue analogs, the cubic structure is maintained even if different metal ions are substituted for one another.

B. Weiss temperature

The sign of θ_c is determined by the superexchange interaction between magnetic centers, i.e., either ferromagnetic or antiferromagnetic. Usually, θ_c is negative for ferrimagnets and positive for ferromagnets. In fact, the θ_c values for ferrimagnetic $Mn_{1.5}^{II}[Cr^{III}(CN)_6]\cdot 7.5\ H_2O$ and ferromagnetic $Ni_{1.5}^{II}[Cr^{III}(CN)_6]\cdot 8\ H_2O$ were -67 K and 72 K, respectively. In $(Nr_x^{II}Mn_{1-x}^{II})_{1.5}[Cr^{III}(CN)_6]\cdot zH_2O$, θ_c increased monotonically from negative to positive values with increasing x (Table I). This variation is proposed to be due not to changes in the magnitudes of the superexchange interactions (J_{NiCr}, J_{MnCr}) but to changes in the weighted average of J_{NiCr} and J_{MnCr} as a function of x. Therefore, the x dependence of θ_c indicates that the macroscopic superexchange interaction mode for the mixed ferro-ferrimagnet was shifting from antiferromagnetic to ferromagnetic.

C. Coercive field

The H_c values for x close to 3/7 were larger than those for other values. In general, the H_c values depend upon the grain size of the sample. However, if the grain sizes are nearly the same, the H_c values are expected to depend on I_s. For example, in the case of hysteresis curves for substances in which cubic crystal anisotropy predominates, H_c is expressed by

$$H_c=\frac{\pi\lambda\sigma}{I_s}, \tag{2}$$

where λ is the magnetostriction and σ is the internal stress.[34] This equation shows that H_c is proportional to $(I_s)^{-1}$. The plots of H_c and $(I_s)^{-1}$ vs x showed a qualitatively similar pattern to that shown in Figs. 6(b) and 6(c). Therefore, we can assume the grain sizes to be constant for the whole x range and the large H_c values at x close to 3/7 to be due to small I_s values.

D. Thermodynamics of spontaneous magnetization

In general, ferromagnets exhibit monotonically increasing magnetization curves with decreasing temperature below T_c. However, in the case of ferrimagnets, Néel envisaged the possibility that saturation magnetization vs temperature curves could be classified into four types according to the shape, i.e., Q, R, P, and N types. The Q and R-type curves exhibit monotonic increases with decreasing temperature, while the P type exhibits a single maximum and the N type exhibits two maxima. Interestingly, under small external magnetic fields, the spontaneous magnetization of materials exhibiting N-type behavior can change sign at a particular temperature (compensation temperature, T_{comp}). In fact, several ferrimagnetic materials exhibiting negative magnetization, e.g., $NiFe_{2-x}V_xO_4$, have been found.[17–20] This phenomenon appears when two sublattice magnetizations due to Fe^{II} ions ($S=5/2$) on the tetrahedral (A) and octahedral (B) sites in the spinel ferrite have different temperature dependences.

Magnetization vs temperature curves below T_c in the $(Ni_x^{II}Mn_{1-x}^{II})_{1.5}[Cr^{III}(CN)_6]\cdot zH_2O$ series exhibited various types of behavior depending on x. The shapes of these curves resemble those of the theoretical curves predicted by

Néel, e.g., type R ($x=0$), type N ($x=0.38$), type P ($x=0.45$), and type Q ($x=1$). However, the model in the Néel theory is composed of two types of sublattice sites. The $(Ni^{II}_xMn^{II}_{1-x})_{1.5}[Cr^{III}(CN)_6]$ series is composed of three sublattice sites. Therefore, we have to analyze the spontaneous magnetization vs temperature curves for $(Ni^{II}_xMn^{II}_{1-x})_{1.5}[Cr^{III}(CN)_6]$ based on a molecular-field model with three types of sublattice sites (Ni, Mn and Cr).[35] In Prussian blue-based magnets, the superexchange interaction between the second-nearest-neighbor sites can be neglected because of their long separation distances (ca 10 Å). Therefore, we need only take into account the superexchange coupling between nearest-neighbor sites. The molecular fields H_{Ni}, H_{Mn} and H_{Cr} acting on the three sublattice sites in $(Ni^{II}_xMn^{II}_{1-x})_{1.5}[Cr^{III}(CN)_6]\cdot 7.5\ H_2O$ are expressed as follows:

$$H_{\mathrm{Mn}}=H_0+n_{\mathrm{MnCr}}M_{\mathrm{Cr}}, \tag{3}$$

$$H_{\mathrm{Ni}}=H_0+n_{\mathrm{NiCr}}M_{\mathrm{Cr}}, \tag{4}$$

$$H_{\mathrm{Cr}}=H_0+n_{\mathrm{CrMn}}M_{\mathrm{Mn}}+n_{\mathrm{CrNi}}M_{\mathrm{Ni}}, \tag{5}$$

where H_0 is the external magnetic field, n_{ij} are the molecular-field coefficients, and M_{Ni}, M_{Mn}, and M_{Cr} are the sublattice magnetizations per unit volume for the Ni, Mn, and Cr sites, respectively. The molecular-field coefficients n_{ij} are related to the exchange coefficients (J_{ij}) by

$$n_{\mathrm{MnCr}}=\frac{2Z_{\mathrm{MnCr}}}{\mu N(g\mu_B)^2}\,J_{\mathrm{MnCr}}, \tag{6}$$

$$n_{\mathrm{NiCr}}=\frac{2Z_{\mathrm{NiCr}}}{\mu N(g\mu_B)^2}\,J_{\mathrm{NiCr}}, \tag{7}$$

$$n_{\mathrm{CrMn}}=\frac{2Z_{\mathrm{CrMn}}}{\lambda N(g\mu_B)^2}\,J_{\mathrm{MnCr}}, \tag{8}$$

$$n_{\mathrm{CrNi}}=\frac{2Z_{\mathrm{CrNi}}}{\lambda N(g\mu_B)^2}\,J_{\mathrm{NiCr}}, \tag{9}$$

where μ_B is the Bohr magneton, Z_{ij} are the numbers of the nearest-neighbor i-site ions surrounding a j-site ion, N is the total number of all types of metal ions per unit volume, and λ and μ represent the mole fractions for the A^{II} cations (total of the mole fractions for Mn^{II} and Ni^{II}) ions and for the Cr^{III} ions, respectively.

If we designate the thermally averaged values of the spins of the Mn, Ni, and Cr ions in their respective sites in the direction of each sublattice magnetization as $\langle S_{\mathrm{Mn}}\rangle$, $\langle S_{\mathrm{Ni}}\rangle$, and $\langle S_{\mathrm{Cr}}\rangle$, the sublattice magnetization can be expressed as follows:

$$M_{\mathrm{Mn}}=\lambda(1-x)Ng\mu_B\langle S_{\mathrm{Mn}}\rangle, \tag{10}$$

$$M_{\mathrm{Ni}}=\lambda xNg\mu_B\langle S_{\mathrm{Ni}}\rangle, \tag{11}$$

$$M_{\mathrm{Cr}}=\mu Ng\mu_B\langle S_{\mathrm{Cr}}\rangle, \tag{12}$$

Substituting Eqs. (6)–(9) and (10)–(12) into (3)–(5), we have

$$H_{\mathrm{Mn}}=H_0+\frac{2Z_{\mathrm{MnCr}}(1-x)J_{\mathrm{MnCr}}}{g\mu_B}\langle S_{\mathrm{Cr}}\rangle, \tag{13}$$

$$H_{\mathrm{Ni}}=H_0+\frac{2Z_{\mathrm{NiCr}}xJ_{\mathrm{NiCr}}}{g\mu_B}\langle S_{\mathrm{Cr}}\rangle, \tag{14}$$

$$H_{\mathrm{Cr}}=H_0+\frac{2Z_{\mathrm{CrMn}}(1-x)J_{\mathrm{MnCr}}}{g\mu_B}\langle S_{\mathrm{Mn}}\rangle+\frac{2Z_{\mathrm{CrNi}}xJ_{\mathrm{NiCr}}}{g\mu_B}\langle S_{\mathrm{Ni}}\rangle, \tag{15}$$

the magnitudes of $\langle S_{\mathrm{Mn}}\rangle$, $\langle S_{\mathrm{Ni}}\rangle$, and $\langle S_{\mathrm{Cr}}\rangle$, setting $H_0=0$, are given by

$$\langle S_{\mathrm{Mn}}\rangle=S_{\mathrm{Mn}\,0}B_{S_{\mathrm{Mn}\,0}}\left(\frac{g\mu_BH_{\mathrm{Mn}}S_{\mathrm{Mn}\,0}}{k_BT}\right)=S_{\mathrm{Mn}\,0}B_{S_{\mathrm{Mn}\,0}}\left(\frac{2Z_{\mathrm{MnCr}}(1-x)J_{\mathrm{MnCr}}S_{\mathrm{Mn}\,0}}{k_BT}\langle S_{\mathrm{Cr}}\rangle\right), \tag{16}$$

$$\langle S_{\mathrm{Ni}}\rangle=S_{\mathrm{Ni}\,0}B_{S_{\mathrm{Ni}\,0}}\left(\frac{g\mu_BH_{\mathrm{Ni}}S_{\mathrm{Ni}\,0}}{k_BT}\right)=S_{\mathrm{Ni}\,0}B_{S_{\mathrm{Ni}\,0}}\left(\frac{2Z_{\mathrm{NiCr}}xJ_{\mathrm{NiCr}}S_{\mathrm{Ni}\,0}}{k_BT}\langle S_{\mathrm{Cr}}\rangle\right), \tag{17}$$

$$\langle S_{\mathrm{Cr}}\rangle=S_{\mathrm{Cr}\,0}B_{S_{\mathrm{Cr}\,0}}\left(\frac{g\mu_BH_{\mathrm{Cr}}S_{\mathrm{Cr}\,0}}{k_BT}\right)=S_{\mathrm{Cr}\,0}B_{S_{\mathrm{Cr}\,0}}\left(\frac{2Z_{\mathrm{CrMn}}(1-x)J_{\mathrm{MnCr}}S_{\mathrm{Cr}\,0}}{k_BT}\langle S_{\mathrm{Mn}}\rangle+\frac{2Z_{\mathrm{CrNi}}xJ_{\mathrm{MnCr}}S_{\mathrm{Cr}\,0}}{k_BT}\langle S_{\mathrm{Ni}}\rangle\right), \tag{18}$$

where B_s is the Brillouin function, $S_{\mathrm{Mn}0}$, S_{Ni0} and $S_{\mathrm{Cr}\,0}$ are the values of $\langle S_{\mathrm{Mn}}\rangle$, $\langle S_{\mathrm{Ni}}\rangle$, and $\langle S_{\mathrm{Cr}}\rangle$ at $T=0$ K, and k_B is the Boltzmann constant. The $\langle S_{\mathrm{Mn}}\rangle$, $\langle S_{\mathrm{Ni}}\rangle$, and $\langle S_{\mathrm{Cr}}\rangle$ can be calculated numerically. The total magnetization (M_{total}) is

$$M_{\mathrm{total}}=-M_{\mathrm{Mn}}+M_{\mathrm{Ni}}+M_{\mathrm{Cr}}=Ng\mu_B[-\lambda(1-x)\langle S_{\mathrm{Mn}}\rangle+\lambda x\langle S_{\mathrm{Ni}}\rangle+\mu\langle S_{\mathrm{Cr}}\rangle]. \tag{19}$$

The negative and positive signs are for antiparallel and parallel interactions, respectively. For $(Ni^{II}_xMn^{II}_{1-x})_{1.5}[Cr^{III}(CN)_6]\cdot 7.5\ H_2O$, the numbers of nearest neighbors Z_{ij} are $Z_{\mathrm{MnCr}}=Z_{\mathrm{NiCr}}=4$, $Z_{\mathrm{CrNi}}=Z_{\mathrm{CrMn}}=6$; and other quantities are as follows: $\lambda=1.5$; $\mu=1$; $S_{\mathrm{Mn}\,0}=5/2$; $S_{\mathrm{Ni}\,0}=1$; $S_{\mathrm{Cr}\,0}=3/2$; and $g=2$.

In order to calculate the temperature dependence, the J values of $Mn^{II}_{1.5}[Cr^{III}(CN)_6]$ and $Ni^{II}_{1.5}[Cr^{III}(CN)_6]$ must be estimated. These values were obtained from the observed T_c values for these compounds. The relationship between the T_c values for the Prussian blue analogs and the J values is expressed as follows:

$$T_c=\frac{2\sqrt{Z_{ij}Z_{ji}}|J_{ij}|}{3k_B}\sqrt{S_i(S_i+1)S_j(S_j+1)}, \tag{20}$$

where i=Ni or Mn and j=Cr. Based on this equation, $J_{\mathrm{NiCr}}=5.6\ \mathrm{cm}^{-1}$ and $J_{\mathrm{MnCr}}=-2.5\ \mathrm{cm}^{-1}$ were obtained, us-

ing T_c values of a 72 K for $Ni^{II}_{1.5}[Cr^{III}(CN)_6]\cdot 8\ H_2O$ and a 67 K for $Mn^{II}_{1.5}[Cr^{III}(CN)_6]\cdot 7.5\ H_2O$. These J values are reasonably close to those for $Mr^{II}-Cr^{III}$ interactions and Ni^{II}-Cr^{III} interactions in heptanuclear $Cr^{III}Mn^{II}_6$ and in $Cr^{III}Ni^{II}_6$ complexes, respectively.

The J_{NiCr} value for the heptanuclear $Cr^{III}Ni^{II}_6$ complex $[Cr\{(CN)Ni(tetraen)_6\}](ClO_4)_9$ is 8 cm^{-1} and the J_{MnCr} value for the heptanuclear $Cr^{III}Mn^{II}_6$ complex $[Cr\{(CN)Mn(trispicMeen)_6\}](ClO_4)_9$ (trispicMeen: N,N,N'-(tris(2-pyridylmethyl)-N'-methyl-ethane)1,2-diamine) is -4 cm^{-1}.[36,37]

For the calculation of magnetization dependences in the $(Ni^{II}Mr^{II}_{1-x})_{1.5}Cr^{III}(CN)_6\cdot zH_2O$ series, the magnetizations of Ni and Cr are expected to be along the direction of the external magnetic field because experimental curves were observed by a field cooling (10 or 1000 G) method and the T_c value for $Ni^{II}_{1.5}[Cr^{III}(CN)_6]$ was higher than that for $Mn^{II}_{1.5}[Cr^{III}(CN)_6]$. Therefore, in this system, the signs of the magnetization of ferromagnetic sites (Ni and Cr) were assumed to be positive. Moreover, the calculated spontaneous magnetizations are essentially the saturated values, because molecular-field theory does not consider the magnetization process. In the experiment, however, the observed magnetization depends on the external magnetic field. The negative magnetization below T_{comp} is compelled to invert along the external magnetic-field direction when the external magnetic field is larger. Therefore, for simulations of observed temperature dependence curves at 10 and 1000 G, the M_{total} and the $|M_{total}|$ curves were adopted, respectively.

Under these conditions, the temperature dependences of the spontaneous magnetization were calculated for several different compositions. For $x=0$, only J_{MnCr} appeared in the equation, and hence the curve exhibited a monotonically increasing magnetization with decreasing temperature. For $0.33<x<3/7$ (0.429), the $|M_{total}|$ curves exhibited two maxima, with a minimum at T_{comp} [see curve for $x=0.38$ in Fig. 7(b)]. This T_{comp} shifted from T_c to 0 K with increasing x. On the other hand, M_{total} for $0.33<x<3/7$ exhibited negative magnetization with T_{comp} [Fig. 8(b)]. For $x=3/7$, T_{comp} was 0 K, and this value corresponds to that predicted by Eq. (1) in which the saturation magnetization disappeared. For $x>0.45$, the curve exhibited a single maximum. For $x=1$, the curve exhibited a monotonic increase due to the fact that only J_{NiCr} appears. The calculated curves for $|M_{total}|$ and M_{total} qualitatively reproduced the experimental ones at 1000 and 10 G, as shown in Figs. 7 and 8, respectively.[38]

These various types of temperature dependence of the magnetization arise because the negative magnetization due to the Mn^{II} sublattice and the positive magnetizations due to the Ni^{II} and Cr^{III} sublattices have different temperature dependences [Fig. 9(a)]. For example, for $x=0.38$, the relations of the magnitude among each sublattice magnetizations were as follows: $|M_{Ni}|+|M_{Cr}|>|M_{Mn}|$ at $T>T_{comp}$ and $|M_{Ni}|+|M_{Cr}|<|M_{Mr}|$ at $T<T_{comp}$, respectively [Fig. 9(b)]. The close correspondence between the calculated and observed curves shows that the magnetic properties of the $(Ni^{II}_xMr^{II}_{1-x})_{1.5}[Cr^{III}(CN)_6]\cdot zH_2O$ series can be predicted using a molecular-field model that considered only superexchange interactions between the nearest neighbors (Ni^{II}-Cr^{III} and Mr^{II}-Cr^{III}). We have succeeded in demonstrating mixed

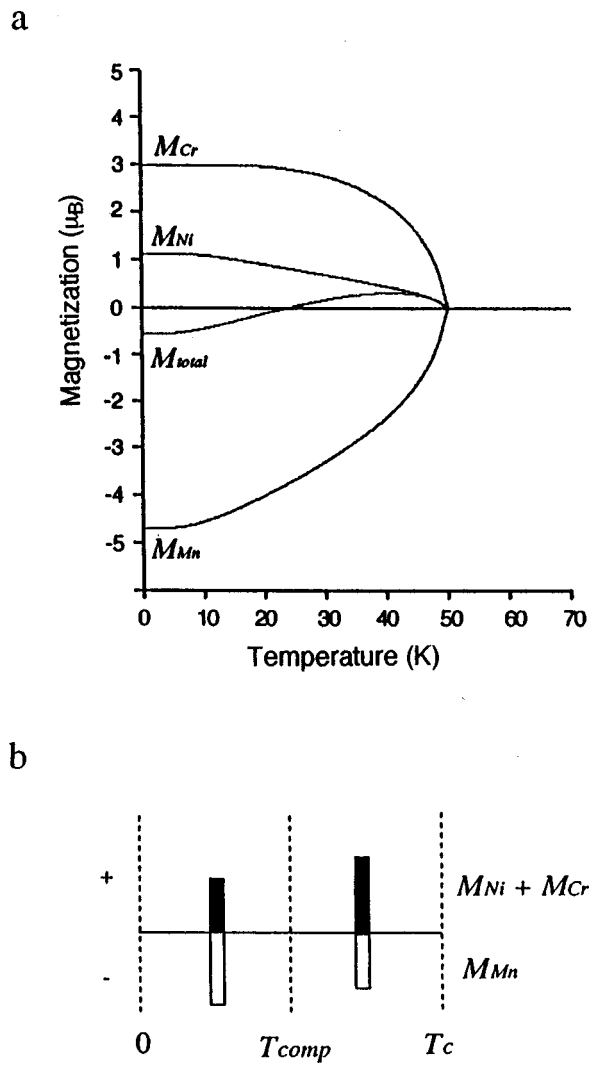

FIG. 9. (a) Calculated temperature dependence curves for each sublattice (M_{Mn}, M_{Ni}, M_{Cr}) and total magnetization (M_{total}) for $(Ni^{II}_{0.38}Mn^{II}_{0.62})_{1.5}[Cr^{III}(CN)_6]$ based on the three-sublattice molecular field theory. (b) Schematic diagram illustrating positive ($M_{Ni}+M_{Cr}$:■) and negative magnetizations (M_{Mn}:□) vs the direction of the external magnetic field at $T>T_{comp}$ and $T<T_{comp}$, respectively.

ferro-ferrimagnetism without spin-glass behavior. One of the main reasons for the success of this model is that the fcc structure of the Prussian blue analogs is maintained even when metal ion substitution is carried out. Another reason is that the superexchange interactions between second-nearest-neighbor sites can be neglected and hence spin frustration does not occur.

VI. CONCLUSIONS

In this work, we prepared molecule-based magnets incorporating both a ferromagnetic ($J>0$) and ferrimagnetic ($J<0$) character in a series of Prussian blue analogs, $(Ni^{II}_xMr^{II}_{1-x})_{1.5}[Cr^{III}(CN)_6]$. The saturation magnetization continuously changed over a wide range as a function of the Ni/Mn ratio. At $x\sim 3/7$, the saturation magnetization disappears, although there is magnetic ordering, and the materials show a drastic increase in coercivity. The Weiss tempera-

tures increased monotonically from negative values to positive values with increasing x, indicating that the predominant interaction mode was shifting from antiferromagnetic to ferromagnetic. In the magnetization vs temperature curves below T_c, all of the various types of temperature dependence curves predicted by Néel, i.e., types R, N, P, and Q, appeared by varying the stoichiometric factor x from 0 to 1. Interestingly, the compounds in which x was in the range $0.38 \leqslant x \leqslant 0.42$ exhibited negative values of magnetization below T_{comp} in a field of 10 G. Our theoretical treatment showed that the various types of behavior for the mixed ferro-ferrimagnets can be represented by molecular-field theory considering only superexchange interactions between nearest-neighbor metal ions. We have succeeded in demonstrating the existence of a novel series of mixed ferro-ferrimagnets without spin-glass behavior.

One of the advantages of molecular magnets compared to conventional ones is that novel types of functionality, for example, control of the magnetic properties via external stimuli, can be incorporated through proper design of the electronic properties. We reported examples of T_c control via electrochemical[4] and optical stimuli,[39–42] using Prussian blue analogs. Moreover, as an example of such an application of the mixed ferro-ferrimagnetism presented in this study, we have recently succeeded in demonstrating a photoinduced magnetic pole inversion using $(Fe_{0.40}Mn_{0.60})_{1.5}[Cr^{III}(CN)_6]$.[24] We expect that compounds in the mixed ferro-ferrimagnet series may also exhibit other types of interesting behavior in addition to magnetic behavior, for example, anomalous conductivity and optomagnetic effects.

ACKNOWLEDGMENTS

We thank N. Sakamoto for technical support and D. A. Tryk for reading the manuscript.

*Present address: Research Center for Advanced Science and Technology, The University of Tokyo 4-6-1 Komaba, Meguro-ku, Tokyo 153, Japan.

†Present address: Department of Industrial Chemistry, Tokyo Metropolitan University, Minami Osawa, hachioji, Tokyo 192-03, Japan.

‡To whom correspondence should be addressed.

[1] J. S. Miller and A. J. Epstein, Angew. Chem. Int. Ed. Engl. **33**, 385 (1994).

[2] O. Kahn, *Molecular Magnetism* (VCH, New York, 1993).

[3] D. Gatteschi *et al.*, *Magnetic Molecular Materials* (Kluwer, Dordrecht, 1991).

[4] O. Sato, T. Iyoda, A. Fujishima, and K. Hashimoto, Science **271**, 49 (1996).

[5] T. Mallah, S. Thiebaut, M. Verdaguer, and P. Veillet, Science **262**, 1554 (1993).

[6] R. E. William and G. S. Girolami, Science **268**, 397 (1995).

[7] S. Ferlay, T. Mallah, R. Ouahés, P. Veillet, and M. Verdaguer, Nature (London) **378**, 701 (1995).

[8] V. Gadet, T. Mallah, I. Castro, and M. Verdaguer, J. Am. Chem. Soc. **114**, 9213 (1992).

[9] W. D. Griebler and D. Babel, Z. Naturforsch. B **87**, 832 (1982).

[10] R. Klenze, B. Kanellakopulos, G. Yrageser, and H. H. Eysel, J. Chem. Phys. **72**, 5819 (1980).

[11] W. R. Entley and G. S. Girolami, Inorg. Chem. **33**, 5165 (1994).

[12] V. Gadet *et al.*, in *Magnetic Molecular Materials*, Vol. 198 of *NATO Advanced Study Institute*, Series E: Physics, edited by D. Gatteschi *et al.* (Kluwer, Dordrecht, 1991), p. 281.

[13] A. Ludi and H. U. Güdel, in *Structure and Bonding*, edited by J. D. Dunitz *et al.* (Springer-Verlag, Berlin, 1973), Vol. 14, p. 1.

[14] H. U. Güdel, H. Stucki, and A. Ludi, Inorg. Chim. Acta **7**, 121 (1973).

[15] S. Ohkoshi, O. Sato, T. Iyoda, A. Fujishima, and K. Hashimoto, Inorg. Chem. **36**, 268 (1997).

[16] L. Néel, Ann. Phys. (Leipzig) **3**, 137 (1948).

[17] E. W. Gorter, Philips Res. Rep. **9**, 295 (1954).

[18] F. K. Lotgering, Philips Res. Rep. **11**, 190 (1956).

[19] R. Pauthenet, J. Appl. Phys. **29**, 253 (1958).

[20] Landolt-Börnstein New Serie III/4b (Springer-Verlag, Berlin, 1970).

[21] C. Mathoniére, C. J. Nuttal, S. G. Carling, and P. Day, J. Chem. Soc. Chem. Commun. **1994**, 1551 ().

[22] C. Mathoniére, C. J. Nuttal, S. G. Carling, and P. Day, Inorg. Chem. **35**, 1201 (1996).

[23] N. Re, E. Gallo, C. Floriani, H. Miyasaka, and N. Matumoto, Inorg. Chem. **35**, 5964 (1996).

[24] S. Ohkoshi, S. Yorozu, O. Sato, T. Iyoda, A. Fujishima, and K. Hashimoto, Appl. Phys. Lett. **70**, 1040 (1997).

[25] J. B. Goodenough, Phys. Rev. **100**, 564 (1959).

[26] J. B. Goodenough, J. Phys. Chem. Solids **6**, 287 (1958).

[27] J. Kanamori, J. Phys. Chem. Solids **10**, 87 (1959).

[28] A. P. Ginsberg, Inorg. Chim. Acta. Rev. **5**, 45 (1971).

[29] M. Verdaguer, T. Mallah, V. Gadet, I. Castro, C. Hélary, S. Thiébaut, and P. Veillet, Conf. Coord. Chem. **14**, 19 (1993).

[30] Analyses: calc. for $Mn_{1.5}[Cr(CN)_6]\cdot 7.5\ H_2O$: Mn, 19.36; Cr, 12.22; C, 16.93; N, 19.75; H_3O, 31.74. Found: Mn, 19.13; Cr, 12.53; C, 16.68; N, 19.42; H_2O, 30.57. Calc. for $(Ni_{0.11}Mn_{0.89})_{1.5}[Cr(CN)_6]\cdot 7.5\ H_2O$: Ni, 2.27; Mn, 17.21; Cr, 12.20; C, 16.91; N, 19.72. Found: Ni, 2.29; Mn, 17.07; Cr, 12.57; C, 17.00; N, 19.43. Calc. for $(Ni_{0.21}Mn_{0.79})_{1.5}[Cr(CN)_6]\cdot 7.5\ H_2O$: Ni, 4.33; Mn, 15.25; Cr, 12.18; C, 16.88; N, 19.69. Found: Ni, 4.24; Mn, 14.94; Cr, 12.92; C, 16.7; N, 9.5. Calc. for $(Ni_{0.38}Mn_{0.62})_{1.5}[Cr(CN)_6\cdot 7.5\ H_2O$: Ni, 7.82; Mn, 11.94; Cr, 12.16; C, 16.85; N, 19.65. Found: Ni, 7.78; Mn, 11.63; Cr, 12.52; C, 17.28; N, 19.68. Calc. for $(Ni_{0.39}Mn_{0.61})_{1.5}[Cr(CN)_6\cdot 7.5\ H_2O$: Ni, 8.02; Mn, 11.75 Cr, 12.15; C, 16.84; N, 19.65. Found: Ni, 7.98; Mn, 11.63; Cr, 12.73; C, 16.72; N, 19.68. Calc. for $(Ni_{0.40}Mn_{0.60})_{1.5}[Cr(CN)_6]\cdot 7.5\ H_2O$: Ni, 8.23; Mn, 11.56; Cr, 12.15; C, 16.84; N, 19.65. Found: Ni, 8.07; Mn, 11.16; Cr, 12.73; C, 16.49; N, 19.38. Calc. for $(Ni_{0.41}Mn_{0.59})_{1.5}[Cr(CN)_6]\cdot 7.5\ H_2O$: Ni, 8.43; Mn, 11.36; Cr, 12.15; C, 16.84; N, 19.64. Found: Ni, 8.33; Mn, 10.88; Cr, 12.67; C, 16.41; N, 19.09. Calc. for $(Ni_{0.42}Mn_{0.58})_{1.5}[Cr(CN)_6]\cdot 7.5\ H_2O$: Ni, 8.64; Mn, 11.17; Cr, 12.15; C, 16.84; N, 19.64. Found: Ni, 8.39; Mn, 11.04; Cr, 12.42; C, 17.04; N, 19.95. Calc. for $(Ni_{0.43}Mn_{0.57})_{1.5}[Cr(CN)_6]\cdot 7.5\ H_2O$: Ni, 8.84; Mn, 10.97; Cr, 12.15; C, 16.83; N, 19.64. Found: Ni, 8.86; Mn, 10.75; Cr, 12.49; C, 16.62; N, 19.45. Calc. for $(Ni_{0.45}Mn_{0.55})_{1.5}[Cr(CN)_6]\cdot 7.5\ H_2O$: Ni, 9.25; Mn, 10.59; Cr, 12.14; C, 16.83; N, 19.63. Found: Ni, 9.08; Mn, 10.51; Cr,

12.60; C, 17.07; N, 19.65. Calc. for $(Ni_{0.48}Mn_{0.52})_{1.5}[Cr(CN)_6]\cdot 7.5\ H_2O$: Ni, 9.87; Mn, 10.00; Cr, 12.14; C, 16.82; N, 19.62. Found: Ni, 9.63; Mn, 9.89; Cr, 12.43; C, 17.22; N, 19.75. Calc. for $(Ni_{0.52}Mn_{0.48})_{1.5}[Cr(CN)_6\cdot 7.5\ H_2O$: Ni, 10.68; Mn, 9.23; Cr, 12.13; C, 16.81; N, 19.61. Found: Ni, 10.65; Mn, 9.24; Cr, 12.71; C, 16.95; N, 19.27. Calc. for $(Ni_{0.62}Mn_{0.38})_{1.5}[Cr(CN)_6\cdot 7.5\ H_2O$: Ni, 12.72; Mn, 7.30; Cr, 12.18; C, 16.79; N, 19.59. Found: Ni, 12.50; Mn, 7.15; Cr, 12.58; C, 16.4; N, 18.9. Calc. for $(Ni_{0.71}Mn_{0.29})_{1.5}[Cr(CN)_6]\cdot 7.5\ H_2O$: Ni, 14.75; Mn, 5.37; Cr, 12.10; C, 16.77; N, 19.56. Found: Ni, 14.56; Mn, 5.39; Cr, 12.64; C, 17.11; N, 19.69. Calc. for $(Ni_{0.81}Mn_{0.19})_{1.5}[Cr(CN)_6]\cdot 7.5\ H_2O$: Ni, 16.58; Mn, 3.64; Cr, 12.09; C, 16.75; N, 19.54. Found: Ni, 15.90; Mn, 3.44; Cr, 12.12; C, 16.4; N, 18.8. Calc. for $Ni_{1.5}[Cr(CN)_6]\cdot 8\ H_2O$: Ni, 20.00; Cr, 11.81; C, 16.37; N, 19.09; H_2O, 32.74. Found: Ni, 19.46; Cr, 11.54; C, 16.36; N, 18.60; H_2O, 32.96.

[31] M.-A. Arrio, Ph. Sainctavit, Ch. Cariter dit Moulin, Vh. Brouder, F. M. F. de Groot, T. Mallah, and M. Verdaguer, J. Phys. Chem. **100**, 4679 (1996).

[32] A. Bencini and D. Gatteschi, *EPR of Exchange Coupled Systems* (Springer-Verlag, Berlin, 1990).

[33] In the case of a metal complex composed of two different metals, the relation between the g value of the complex and those of each metal is as follows: $g=(1+c)/2g_A+(1-c)/2g_B$, $c=S_A(S_A+1)-S_B(S_B+1)/S(S+1)$, where g_A is g_{Mr}. Based on this equation, the g_{Mn} value was estimated from the g_{Cr} value and the EPR data for $Cs^{II}Mn^{II}[Cr^{III}(CN)_6]$.

[34] S. Chikazumi, *Physics of Magnetism* (Wiley & Sons, New York, 1964), p. 357.

[35] E. E. Anderson, in *Proceedings of the International Conference on Magnetism* (Institute of Physics and The Physical Society, London, 1965), p. 660.

[36] T. Mallah, C. Auberger, M. Verdaguer, and P. Veillet, J. Chem. Soc. Chem. Commun. **1995**, 61.

[37] A. Scuiller, T. Mallah, M. Verdaguer, A. Nivorozkhin, J. L. Tholence, and P. Veillet, New J. Chem. **20**, 1 (1996).

[38] For x close to 0 and 1, the calculated curves for $|M_{\mathrm{total}}|$ reproduce the experimental curves at 1000 G to a good approximation in both magnetization and T_c. However, the experimental magnetization values as a function of temperature curves for $x\sim 3/7$ $(=0.429)$ are smaller than the calculated ones. One of the reasons for this is that the magnetization for x close to 3/7 cannot be saturated at 1000 G because the coercive fields are larger than those for $x=0$ and 1 (see Fig. 7). For example, H_c is 680 G for $x=0.42$ (see Table I). Moreover, the observed T_c value is higher than that of the calculated one. Experimental T_c values are almost constant for the whole x range, although they are expected to sink at $x=3/7$ from the results of the calculation. We are now investigating this difference between calculated and observed T_c.

[39] O. Sato, T. Iyoda, A. Fujishima, and K. Hashimoto, Science **272**, 704 (1996).

[40] O. Sato, Y. Einaga, T. Iyoda, A. Fujishima, and K. Hashimoto, J. Electrochem. Soc. **144**, L11 (1997).

[41] Y. Einaga, O. Sato, T. Iyoda, Y. Kobayashi, F. Ambe, K. Hashimoto, and A. Fujishima, Chem. Lett. **1997**, 289.

[42] K. Nagai, T. Iyoda, A. Fujishima, and K. Hashimoto, Solid State Commun. **102**, 809 (1997).